A Framed Monochromatic X-Ray Microscope for ICF

The Laser Fusion Experiments Groups from the Laboratory for Laser Energetics (LLE) and the Los Alamos National Laboratory (LANL) have jointly developed an instrument capable of simultaneously space-, time-, and spectrally resolving x-ray emission from inertial confinement fusion (ICF) targets. Uses of the instrument include framed imaging of line emission from fuel or shell dopants and monochromatic backlighting. The x-ray imaging is accomplished with a Kirkpatrick-Baez (KB)–type four-image microscope (developed at LLE). The microscope has a best spatial resolution of ~5 μm and a sensitive energy range of ~2 to 8 keV. Time-resolved x-ray images are obtained with a pair of custom framing cameras (developed at LANL), each of which records two of the four images in two independent 80-ps time intervals. In addition, the energy range of the images can be restricted to a narrow (monochromatic) spectral range (~10 to 100 eV) by the introduction of diffracting crystals. This technique has been demonstrated in LLE's x-ray laboratory with an *e*-beam-generated dc x-ray source, and at the LANL Trident laser facility with x rays from a laser-produced plasma. The microscope and gated monochromatic x-ray imaging (GMXI) module are undergoing initial testing on LLE's OMEGA laser fusion facility.

This instrument accomplishes monochromatic imaging by introducing diffracting crystals near the image plane of the microscope.[1] The arrangement is shown in Fig. 66.6. The microscope optic is a distance d from the source of x-ray emission (target). If a crystal is placed in front of the image plane at a mean angle of θ, the emission within a region Δx and at a wavelength λ will be diffracted, where $\Delta x = d \cdot \Delta\theta$ and $\Delta\theta$ is the rocking curve width of the diffracting crystal. The mean wavelength is given by the Bragg equation $n\lambda = 2d \sin\theta$, where n is the diffraction order and d is the crystal plane spacing. The combination of KB-optic distance (~200 mm) and mosaic crystal rocking-curve width (~0.2°) makes this technique applicable to laser-fusion plasmas (since in this case Δx ~ 700 μm). The range of energies in the diffracted image is $\Delta E = E \cot\theta \cdot \Delta\theta$. An additional consequence of using the diffracting crystal is a degradation in image quality. This is quantified by considering rays in the microscope near the image plane. The crystal acts as a reradiator, taking an input ray and diffracting it into a spread of angles $\Delta\theta$ that result in a spread of positions $\Delta x'$ at the image plane. Scaling this to the target plane ($\Delta x = \Delta x'/M$, where M is the magnification) and noting that $\Delta x' = \Delta z \cdot \Delta\theta$, where Δz is the separation between the crystal and the detector, gives an image smearing of $\Delta s = \Delta z \cdot \Delta\theta / M$. This quantity can be minimized for a given $\Delta\theta$ by working at large magnification and by working at small crystal-image plane separations (hence the choice of crystal location). An example of resultant smearing for $\Delta\theta \sim 0.2$, $\Delta z =$ 2 cm, and $M = 13.6$ (appropriate to the current design) is $\Delta s \sim$ 5 μm, which is of the order of the best resolution of the KB optics.[1] The arrangement of framing cameras and crystal monochromators that has been adopted for the GMXI is shown in Fig. 66.7.

In order to effectively use this technique to obtain gated monochromatic x-ray images of laser-fusion targets, the microscope, monochromator, and framing cameras have been

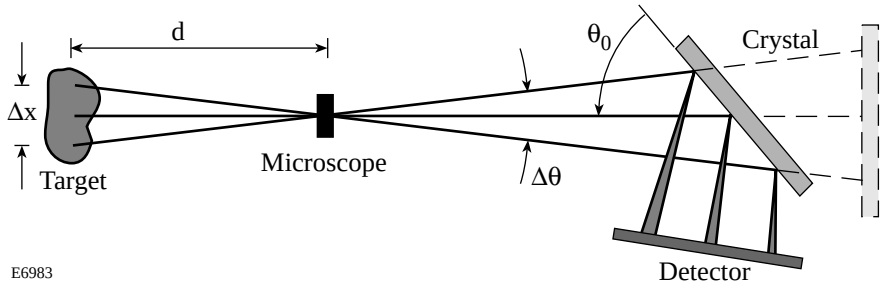

Figure 66.6
Schematic of the technique used to obtain monochromatic x-ray images with a KB microscope.

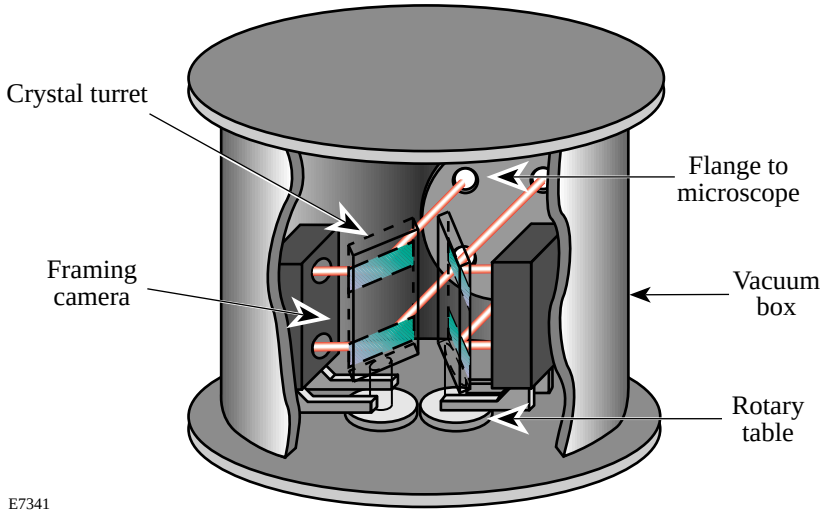

Figure 66.7
The GMXI module consists of two rotary stages, each of which positions a crystal turret-framing module pair. The crystal turrets, each containing two crystals, are positioned at the desired Bragg angle θ_B, while the framing modules are positioned at the diffracted image plane.

individually calibrated and then tested as an integrated system. Figure 66.8 shows the measured resolution of the microscope versus distance from best focus for an individual image. The resolution is seen to approach the ideal resolution calculated by ray tracing. The microscope reflectivity was measured also with a dc x-ray source using the method described in Dhez *et al.*[2] Both the Au-coated and Ir-coated optics have been characterized (Fig. 66.9). Both coatings were produced by ion-assisted deposition and final substrate roughness measured to be ≲4 to 5 Å rms.[3] Figure 66.9(a) shows that the reflectivity of the Au-coated mirrors is in close agreement to that calculated from tabulated values of the atomic scattering factors. The current Ir-coated mirrors show a falloff compared to ideal reflectivity at high energies [Fig. 66.9(b)] (likely due to an underdense coating).[4] Nevertheless, the current Ir-coated mirrors perform as well as the Au-coated mirrors.

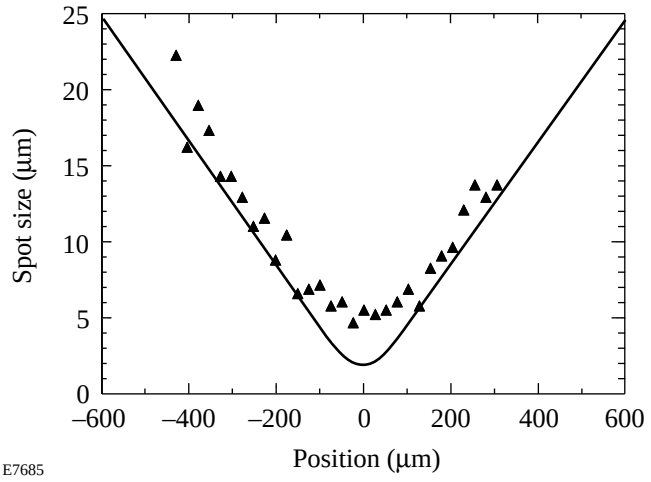

Figure 66.8
Results of resolution measurements of the KB microscope mirror assembly. The spot size (full width) versus position from best focus was determined from a backlit image of a Cu-mesh using a dc x-ray source. The solid line is the predicted spot size determined from ray tracing.[1]

Monochromatic imaging with a KB microscope was first demonstrated in the laboratory with a dc x-ray source. Figure 66.10 shows the spectrum of the *e*-beam-generated x-ray source (Ti target) as obtained with a Si(Li) detector. The source was backlighting a grid placed at the focal plane of the KB microscope. A LiF crystal (200 plane, $2d$ = 4.027 Å) was placed 2 cm before the image plane and set to the nominal Bragg angle θ_B for Ti Kα (2.75 Å = 4.51 keV, θ_B = 43.07°). The diffracted spectrum consisting of the single Ti Kα line is also shown in Fig. 66.10. The diffraction peak was then scanned about this nominal central angle in order to verify the accuracy of angular alignment. Once the angle of peak reflectivity was found, a film pack was placed in front of the Si(Li) detector at the image plane. Figure 66.11 shows the results of these experiments. Monochromatic images were taken of Ti Kα emission with a LiF crystal and with a highly oriented pyrolytic graphite (HOPG) crystal ($2d$ = 6.708 Å, θ_B = 24.20°). As expected, some image degradation resulted. Nevertheless, good quality images were obtained with both crystals.

In a separate set of measurements with the same x-ray source, the diffraction response of LiF and HOPG (rocking curves) was measured by impinging a narrow beam ($\Delta\theta$ < 0.01°) on the crystal. Figure 66.12 shows reflectivity curves for

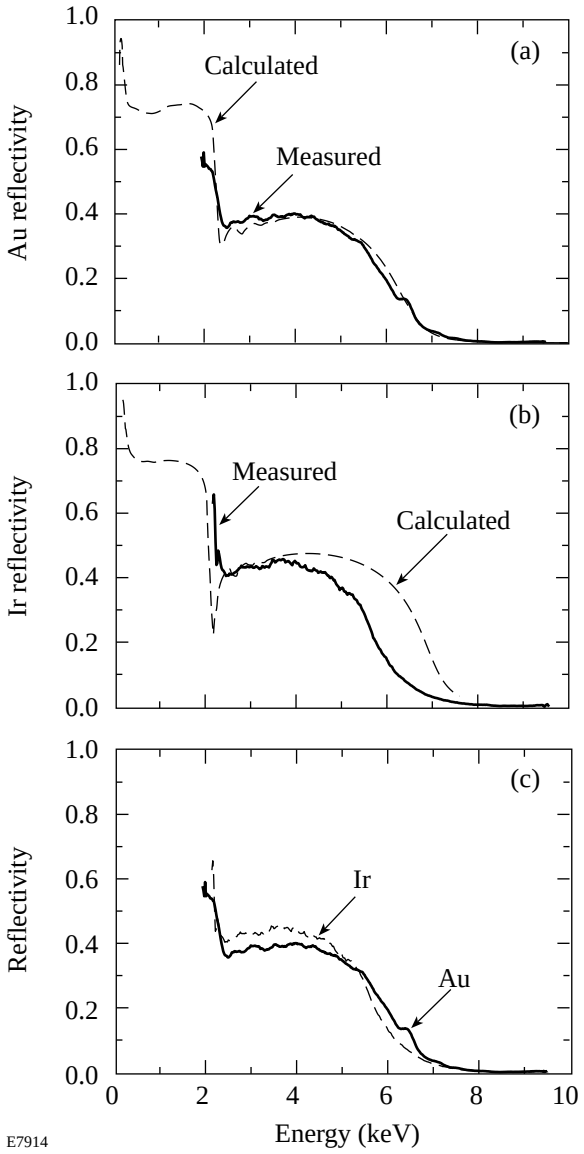

Figure 66.9
X-ray reflectivity measurements of Au- and Ir-coated KB microscope optics.

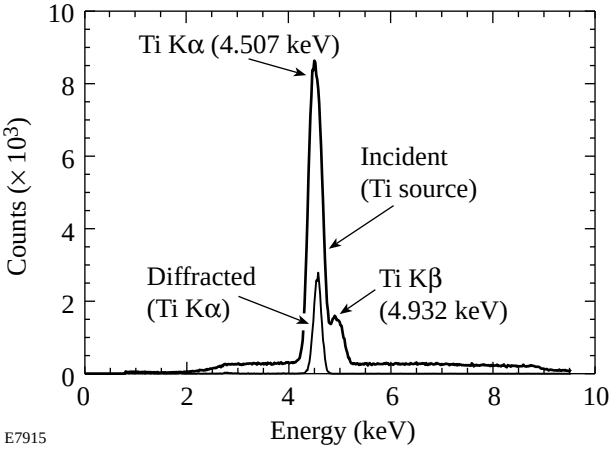

Figure 66.10
The *e*-beam-generated x-ray source and KB-microscope-imaged, diffracted x-ray spectra. Only the Ti Kα line is diffracted by the LiF crystal.

LiF and HOPG both at the Ti Kα line energy. The full-width at half-maximum (FWHM) and peak reflectivities R_p were found to be FWHM = 0.20°, R_p = 0.14 for LiF, and FWHM = 0.55°, R_p = 0.28 for HOPG. The narrower angular response of the LiF crystal yields a higher resultant resolution (~8 μm) but can be seen to limit the field of view (~700 μm) in the plane of crystal diffraction (horizontal axis). Conversely, the HOPG crystal yields a lower spatial resolution (~12 μm) but benefits from a larger field of view (~1400 μm). Both of these tests were performed at an image magnification of 9.3, and the resultant image smearing could be further reduced by operating at higher magnification.

Monochromatic imaging of a laser plasma with a KB microscope was first demonstrated at the LANL Trident laser facility. A Cu mesh was backlit by a Ti disk irradiated by ~150 J of 532-nm light in a 1.2-ns (FWHM) pulse. Figure 66.13 shows the results of these experiments—both broadband [Fig. 66.13(a)] and monochromatic [Fig. 66.13(b)] images were obtained. The monochromatic image is of the

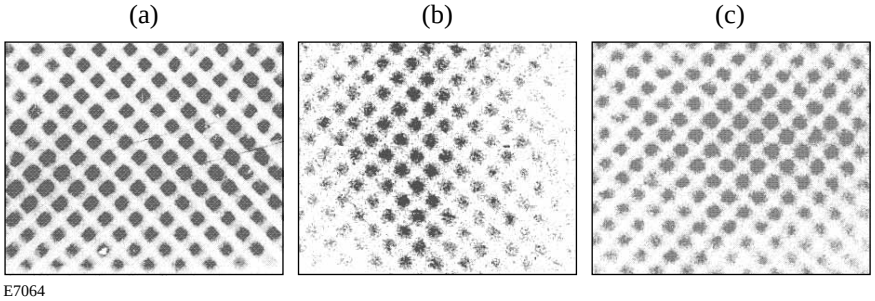

Figure 66.11
Broadband and monochromatic images of backlit grids obtained with a KB microscope and an *e*-beam-generated Ti x-ray source: (a) broadband and monochromatic images of Ti Kα emission taken with a (b) LiF crystal, and (c) HOPG crystal.

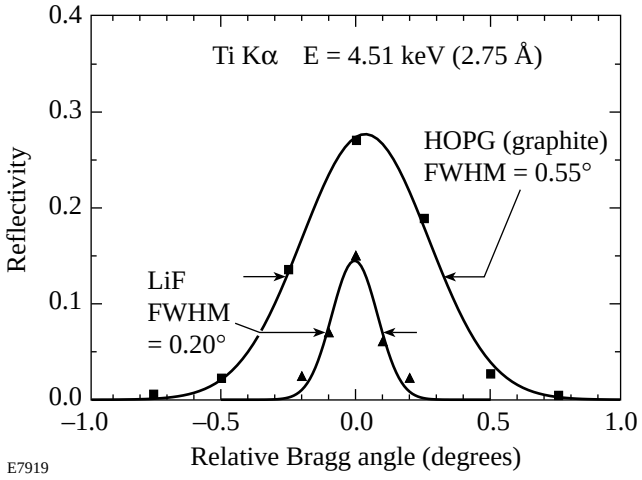

Figure 66.12
Rocking curves for HOPG and LiF at 4.51 keV = 2.75 Å.

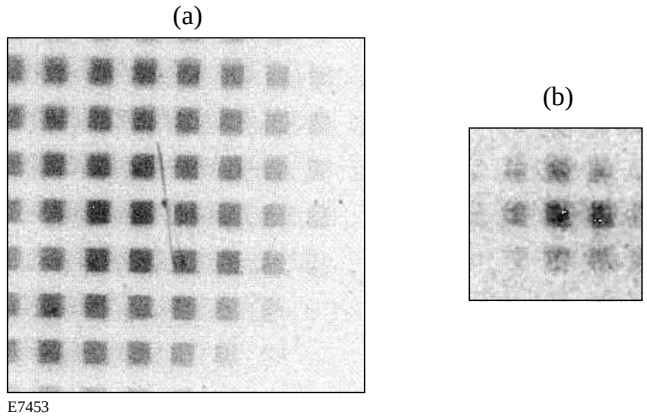

Figure 66.13
KB microscope images of 25-μm wire meshes backlit by Ti disks acquired at the LANL Trident laser facility: (a) broadband (2 to 7 keV), (b) monochromatic [4.75 keV (2.61 Å)].

Ti He-like Ly α line taken with a LiF crystal (2.610 Å = 4.750 keV, $\theta_B = 40.41°$). (In this experiment the magnification was 12.9 and the crystal-image plane separation was 2 cm.) Good resolution was obtained (~10 μm) despite some misalignment of the KB microscope from its optimum focusing position.

Framed images are obtained with a pair of custom modules (developed at LANL), consisting of a pair of 25-mm-diam microchannel plates (MCP's) with proximity-focused fiber-optic faceplates coated with P11 phosphor (Fig. 66.14). Light from the phosphor is recorded by Kodak TMAX film loaded into film packs that press the film against the fiber-optic faceplate. Details of the electronics are described by Oertel *et al.*[5] The current modules have a sensitive frame time of ~80 ps, and the frames on each module are separated by 350 ps (53-mm spatial separation). Each module can be independently gated, providing for flexibility in the type of measurements obtained.

The monochromators consist of a combined crystal turret and detector turret. A geared mechanism drives the detector turret at twice the angle of the crystal turret. A pair of stepper-motor-driven rotary stages drive the turret assemblies. Each turret assembly can be set at a separate angle, allowing two wavelengths to be imaged if desired. The rotary stage angles were calibrated at the Ti Kα energy with both LiF and HOPG crystals by placing a proportional counter at the position of the framing modules on the detector turret. The positions were referenced to the rotary-stage position encoders to an accuracy of 0.01°. The current rotary-stage assemblies can be set to diffraction angles of up to $\theta_B \sim 65°$. The requirement that the diffracted image be away from the direct line of site places a practical lower limit of $\theta_B \sim 15°$. The resulting wavelength range that can be accessed by the GMXI is 1.74 to 6.08 Å (2.04 to 7.12 keV) for HOPG and 1.04 to 3.65 Å (3.40 to

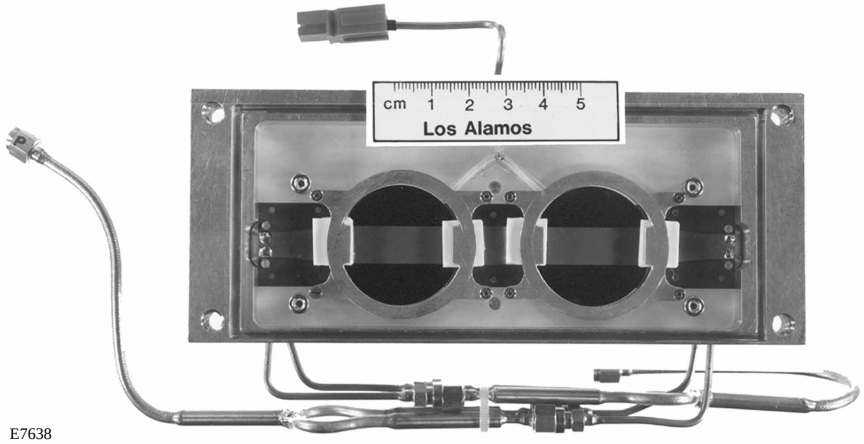

Figure 66.14
The LANL framing camera modules that are used in the GMXI.

11.92 keV) for LiF. [The practical upper limit is further restricted by the mirror reflectivity to ~7 keV (1.8 Å).] These two crystal types are seen to be appropriate to the energy range of the microscope (~2 to 8 keV). The energy band of the diffracted images depends on the crystal angle and type. The LiF crystal provides a narrow band that varies from ~15 eV at 3.4 keV to ~50 eV at 7 keV. The HOPG crystals yield a band of ~10 eV at 2 keV to ~250 eV at 7 keV. Elements whose principal emission lines fall in this range include Si, P, S, Cl, Ar, K, Ca, Sc, Ti, V, Cr, Mn, and Fe.

Figure 66.15 shows a schematic of the KB microscope and GMXI attachment as deployed on OMEGA. A pedestal supports the GMXI assembly. Fine adjustment of the KB microscope pointing is accomplished by raising or lowering the adjustable support legs and by right or left adjusting screws. A referenced pointing adjustment system is built into the microscope and consists of a flexible weldment re-entrant into the OMEGA target chamber, combined with a pair of micrometers that measure the flight tube position. Initial alignment is accomplished by placing a pointer on the end of the microscope's optic blast-shield cover. The pointer is aligned to the target chamber center (TCC) by positioning the GMXI assembly and by a fine adjustment on the optic distance. Film packs containing Kodak DEF were placed at the image plane with the crystal turret removed. After the first image was obtained, final alignment was accomplished by adjusting the GMXI module using the micrometer readings as a reference.

First results of the GMXI were obtained on OMEGA target experiments investigating burnthrough and mix. (Details of this type of experiment are given in Ref. 6.) The targets consisted of DD-filled CH shells with overcoated layers of chlorinated and unchlorinated parylene. Figure 66.16 shows the resultant time-integrated images obtained with an adjoining KB microscope on shot 6483. The broadband time-integrated image shows shell emission plus a bright core, which may contain chlorine ion line emission. Figure 66.17 shows the GMXI results. Framed images were obtained with one module set to look at broadband emission (no crystal monochromator) [Figs. 66.17(a) and 66.17(b)], while a time-integrated monochromatic image was obtained by placing a DEF film pack on the detector turret with an HOPG crystal set to diffract Cl-He–like Ly α emission (4.44 Å = 2.79 keV, θ_B = 41.44°) [Fig. 66.17(c)]. The framed images reveal a target shell early in the implosion [Fig. 66.17(a)] and 350 ps later [Fig. 66.17(b)], at a time near peak compression. The image of the target core in Fig. 66.17(b) is nearly saturated, obscuring fine details of the emission. Conversely, the narrow energy band of the monochromatic image [Fig. 66.17(c)] has further limited the flux to

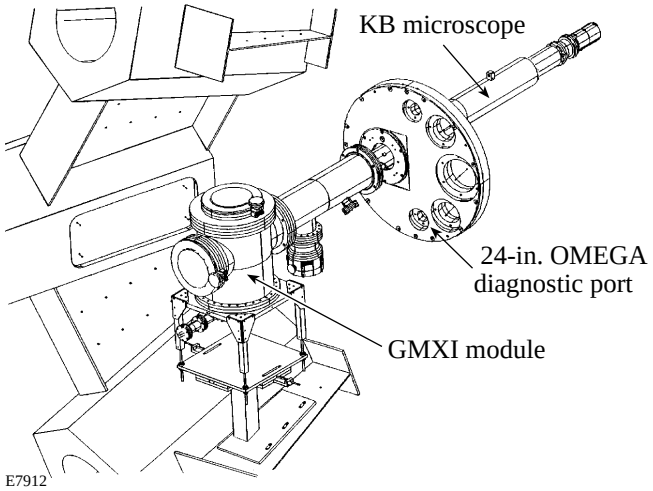

Figure 66.15
Perspective view of the gated monochromatic x-ray microscope (GMXI) as it is deployed on OMEGA.

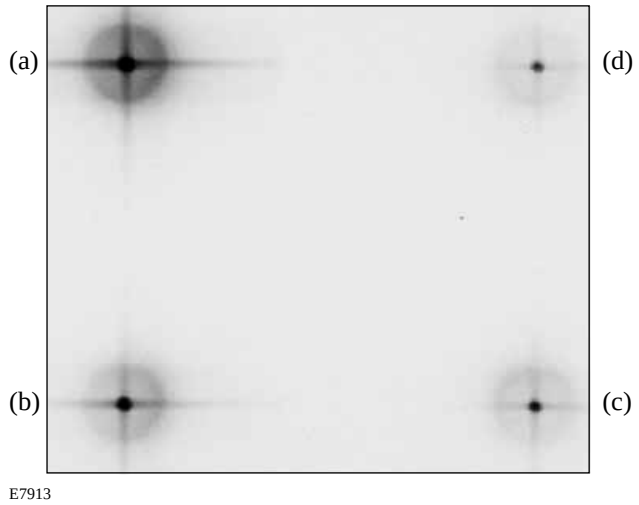

Figure 66.16
Four images obtained with a nearly duplicate KB microscope on OMEGA shot 6483. This microscope viewed the target plane from a nearby direction (~30° away). The four different images are filtered to give a range of exposures. The effective energy bands are (a) 4 to 8 keV, (b) 4.5 to 8 keV, (c) 5 to 8 keV, and (d) 5.5 to 8 keV.

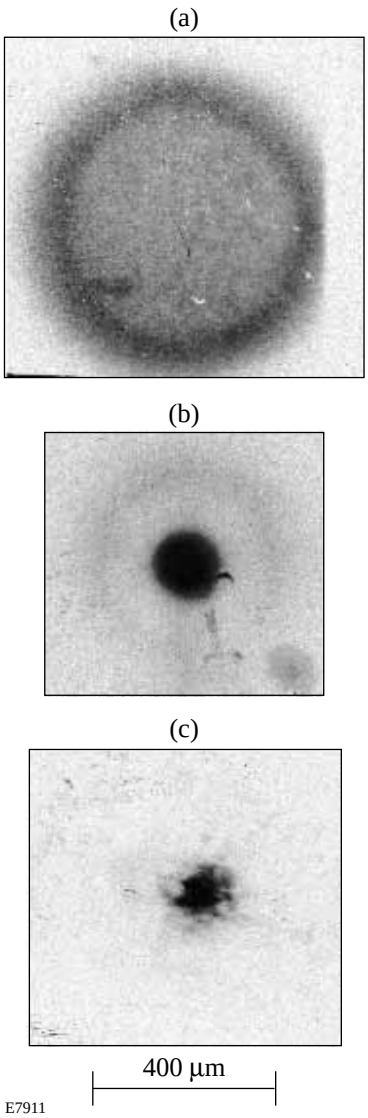

Figure 66.17
Images obtained with the GMXI of an imploding target on OMEGA shot 6483. Framed images were obtained with one module set for broadband imaging (a,b), while a time-integrated monochromatic image of 4.45-Å Cl emission was obtained with an HOPG crystal and a film pack (c). All images have the same scale (indicated by the 400-μm bar).

a level where an unsaturated image was obtained. The calculated energy band of the image ($\Delta E = E \cot\theta \cdot \Delta\theta$) is ~30 eV. The strength of the emission, its size, and location make it unquestionably Cl (He-α). The presence and amount of Cl emission in the core can serve as a diagnostic of mixing.[7]

In conclusion, we have deployed a new diagnostic on the OMEGA target chamber. It is capable of simultaneously space-, time-, and spectrally resolving x-ray emission from laser targets. The project is a collaborative effort between the University of Rochester's Laboratory for Laser Energetics and the Los Alamos National Laboratory. This imaging system will be important in diagnosing shell and core size, density, and mixing in ICF experiments conducted on the OMEGA laser system.

ACKNOWLEDGMENT

The authors acknowledge the support of the staffs at LLE and LANL, and the operations staffs at the LANL Trident laser facility and the LLE OMEGA laser facility. This work was supported by the U.S. Department of Energy Office of Inertial Confinement Fusion under Cooperative Agreement No. DE-FC03-92SF19460, the University of Rochester, and the New York State Energy Research and Development Authority. The support of DOE does not constitute an endorsement by DOE of the views expressed in this article.

REFERENCES

1. F. J. Marshall and Q. Su, Rev. Sci. Instrum. **66**, 725 (1995).
2. P. Dhez, H. Duval, and J. C. MacLaurent, J. X-Ray Sci. Technol. **3**, 176 (1992).
3. D. Smith, LLE (private communication).
4. R. F. Elsner, S. L. O'Dell, and M. C. Weisskopf, J. X-Ray Sci. Technol. **3**, 35 (1991).
5. J. A. Oertel, T. Archuleta, L. Clark, S. Evans, A. Hauer, C. G. Peterson, T. Sedillo, C. Thorn, R. G. Watt, and F. J. Marshall, in *Ultrahigh- and High-Speed Photography, Videography, and Photonics '95*, edited by D. R. Snyder and G. A. Kyrala (SPIE, Bellingham, WA, 1995), Vol. 2549, p. 82.
6. Laboratory for Laser Energetics LLE Review **64**, NITS document No. DOE/SF/19460-99, 1995 (unpublished), p. 160.
7. B. Yaakobi, F. J. Marshall, Q. Su, and R. Epstein, J. X-Ray Sci. Technol. **5**, 73 (1995).